

Supporting Information: Sampling conformational changes of bound ligands using Nonequilibrium Candidate Monte Carlo

Sukanya Sasmal,[†] Samuel C. Gill,[‡] Nathan M. Lim,[†] and David L. Mobley^{*,†,‡}

[†]*Department of Pharmaceutical Sciences, University of California, Irvine*

[‡]*Department of Chemistry, University of California, Irvine*

E-mail: dmobley@mobleylab.org

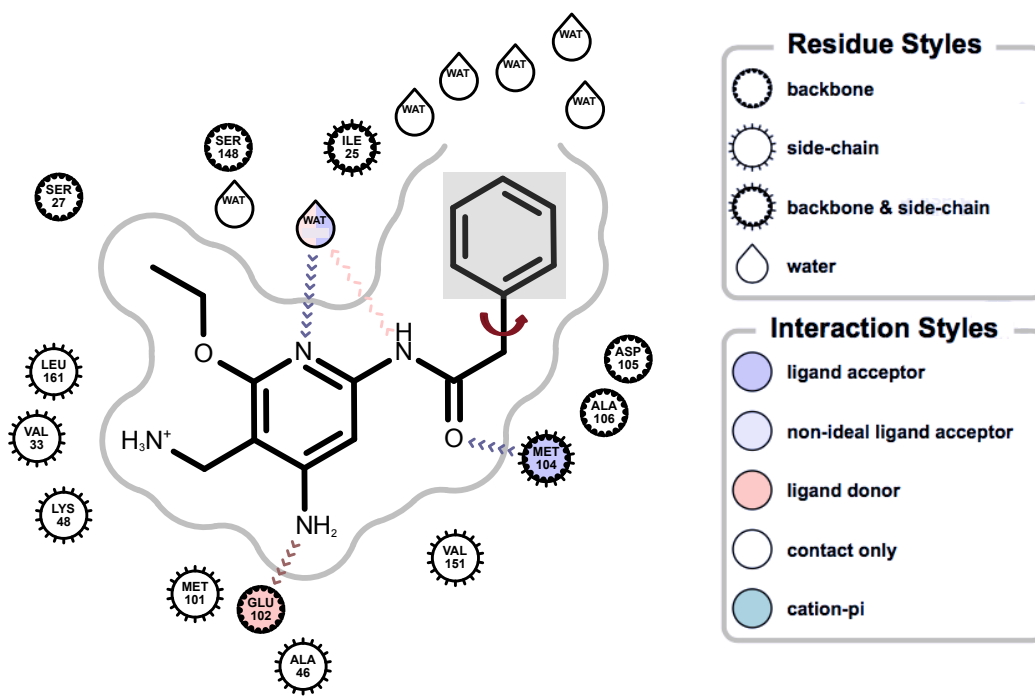


Figure S1. Protein-ligand interaction map showing the important interactions established by ligand **1** in the binding pocket. The alchemical region is shown in gray and the red arrow indicates the rotatable bond. In order to obtain a successful NCMC move proposal for this ligand, the residues Ile25, Asp105 and Ala106, and the adjacent water molecules need to relax accordingly. The non-alchemical region of the ligand maintains its pose during the simulations and has an average heavy-atom RMSD of 1.1 Å with respect to the starting pose. For ligand **2** and **3**, the amount of relaxation required is larger than that by ligand **1** due to the methyl substitution(s) in the phenyl ring. The graphics was generated using OpenEye Toolkits (OpenEye Scientific Software Inc.).

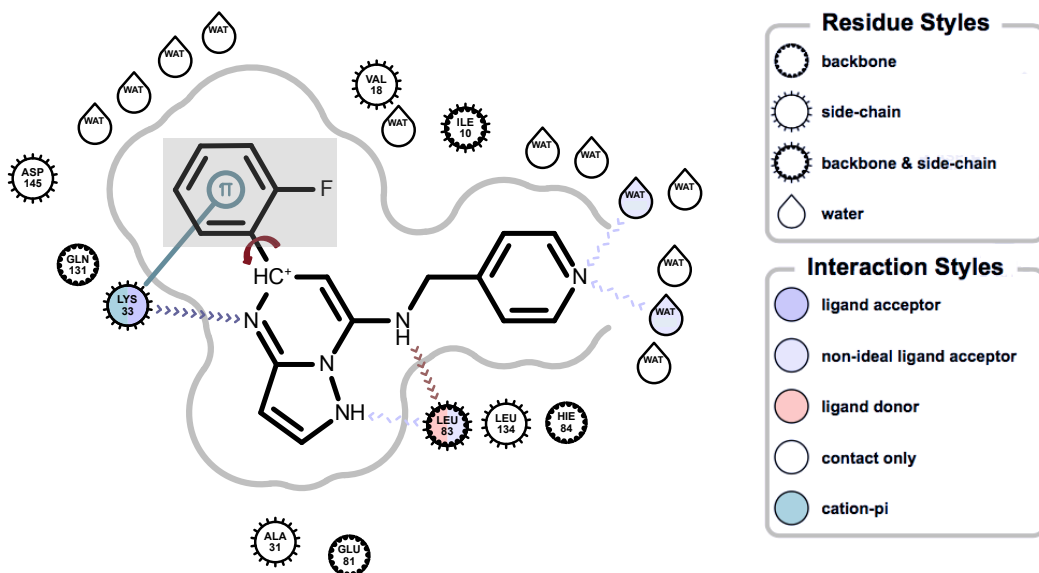


Figure S2. Protein-ligand interaction map showing the important interactions established by ligand 4 in the binding pocket. The alchemical region is shown in gray and the red arrow indicates the rotatable bond. In order to obtain a successful NCMC move proposal for this ligand, the residues Lys33, Gln131 and Asp145, and the adjacent water molecules need to relax accordingly. The graphics was generated using OpenEye Toolkits (OpenEye Scientific Software Inc.).

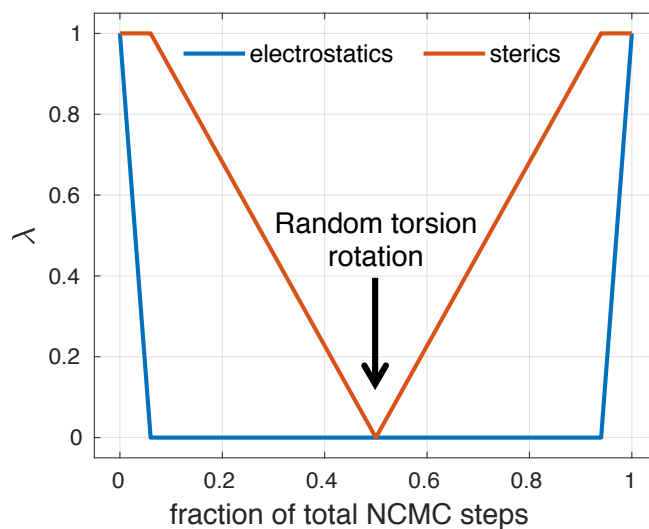


Figure S3. Scaling of the electrostatics and Lennard-Jones forces in the alchemical region of the ligand with respect to λ during the course of a NCMC move proposal. At $\lambda = 0$, the non-bonded interactions are completely turned off, while at $\lambda = 1$, the interactions are fully on. Adapted from Gill et al.¹

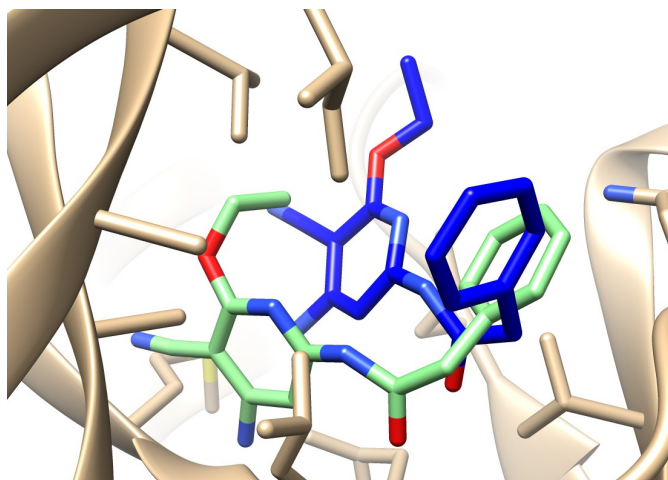


Figure S4. Orientation of the ligand in the binding pocket in two different windows during umbrella sampling simulations - i) **Blue** – window where the flexible bond is restrained to the same value as the stable pose, also the starting pose in the MD and MD/NCMC simulations. ii) **Green** – where the flexible bond is restrained to be at an angle of 90° with respect to the starting orientation. The binding pose of the ligand gets altered in the second case. Hence, we decided to put additional positional restraints on the fixed part of the ligand in all of the windows to prevent the ligand from exploring other binding modes.

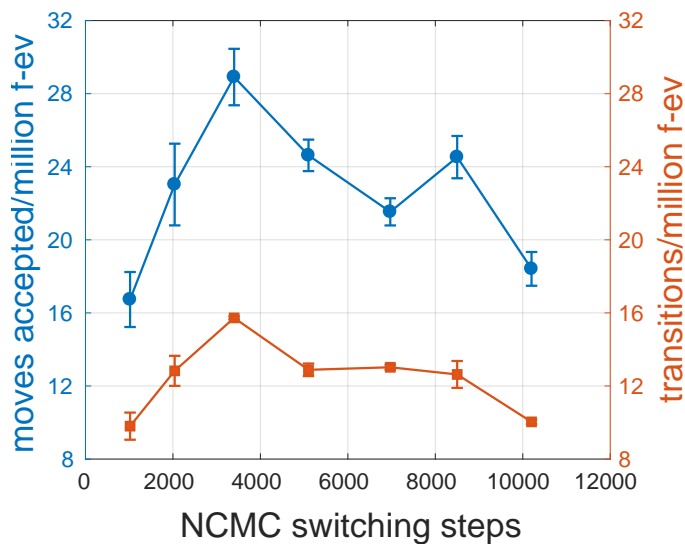


Figure S5. Moves accepted per million force evaluations (f-ev) during MD/NCMC simulation and transitions between different binding poses per million force evaluations (f-ev) as a function of the number of NCMC switching steps for ligand **1**. Accepted moves does not always result in a transition, as seen from the lower values of transitions/million f-ev.

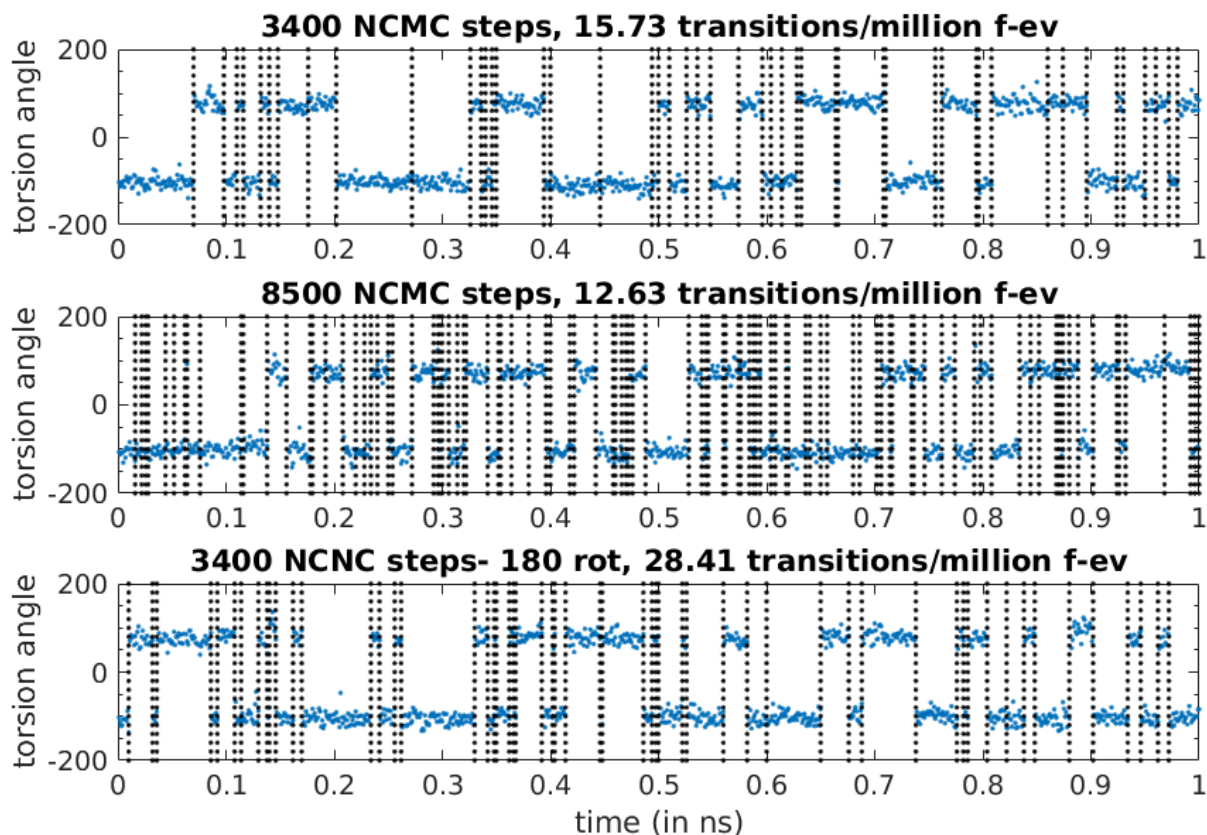


Figure S6. Torsion angles (corresponding to the two binding modes) as a function of time simulated with different NCMC protocols for ligand **1** - 3400 NCMC steps (*top*) and 8500 NCMC steps (*middle*) with random rotational moves; 3400 NCMC steps with random 180° rotational moves (*bottom*). Black dotted vertical lines show the accepted NCMC moves. Not all accepted moves result in a transition between the two binding modes for random rotational moves. For example, during the first 0.1 ns of NCMC simulation in *middle*, moves were accepted, but did not correspond to a successful transition. However, with 180° rotational moves, almost every accepted move resulted in a transition with almost two times increase in the transitions per million force evaluations (transitions/million f-ev).

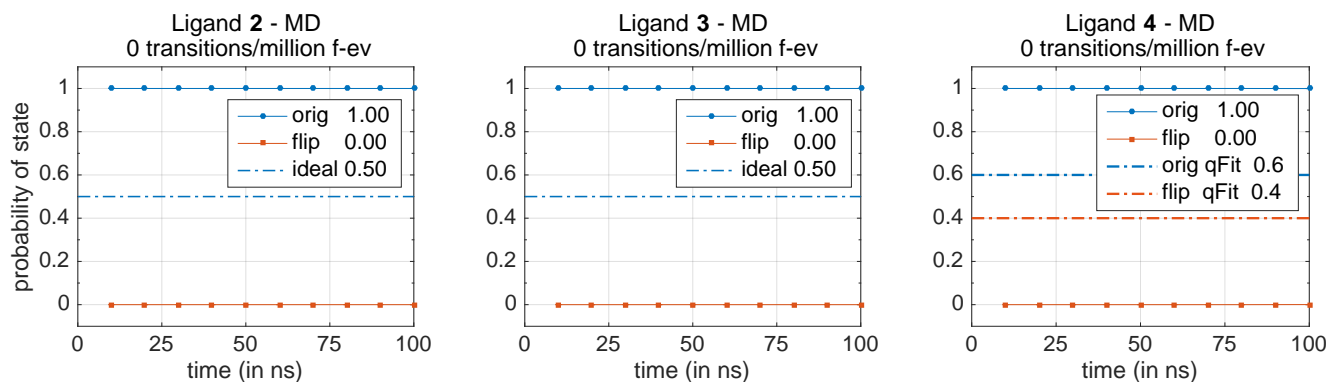


Figure S7. Probability of the binding states of ligands **2**, **3** and **4** as a function of time based on MD simulations (solid lines). The dotted lines show the expected probabilities based on FEP² and qFit³ calculations. We did not observe any transition between the two states for all of the three ligands.

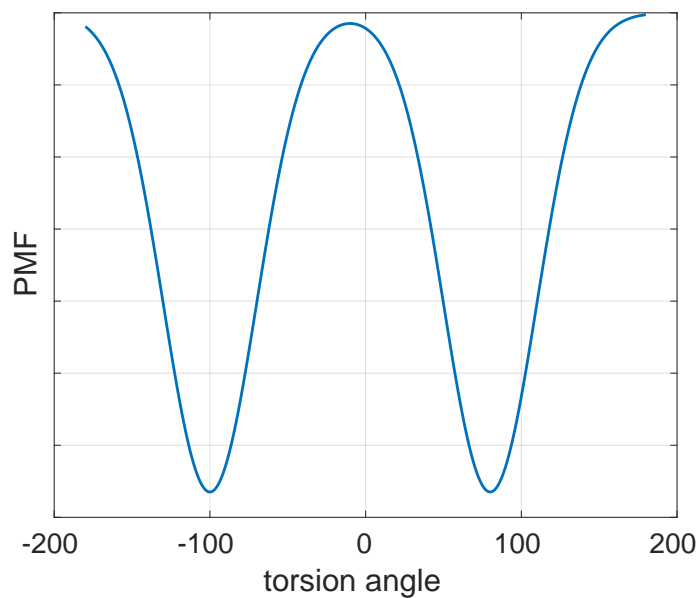


Figure S8. The ‘ideal’ PMF as a function of the torsion angle of the rotatable bond present in ligand **1**. There should be two basins of same depth corresponding to the two identical, but distinct binding modes.

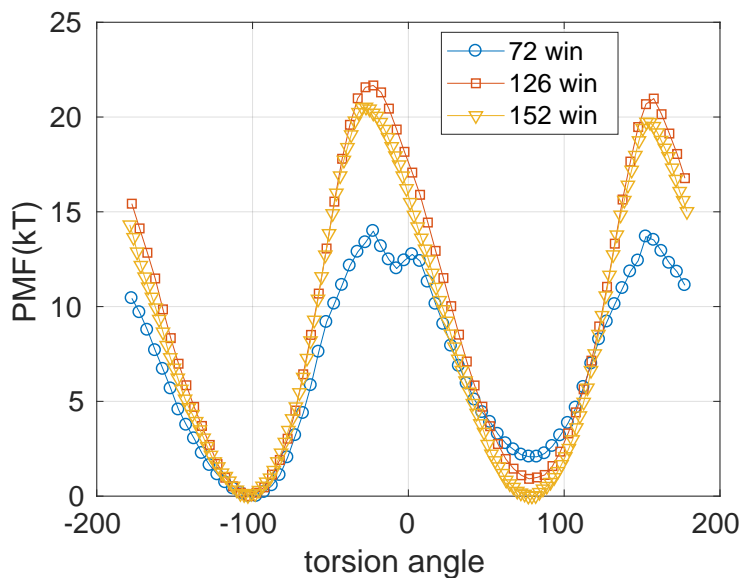


Figure S9. PMF as a function of the torsion angle of the rotatable bond present in ligand **1**, obtained using umbrella sampling simulations. The different parameters used are described in the methods section. We had to use 152 windows to obtain a PMF close to the ‘ideal’ one in Figure S8.

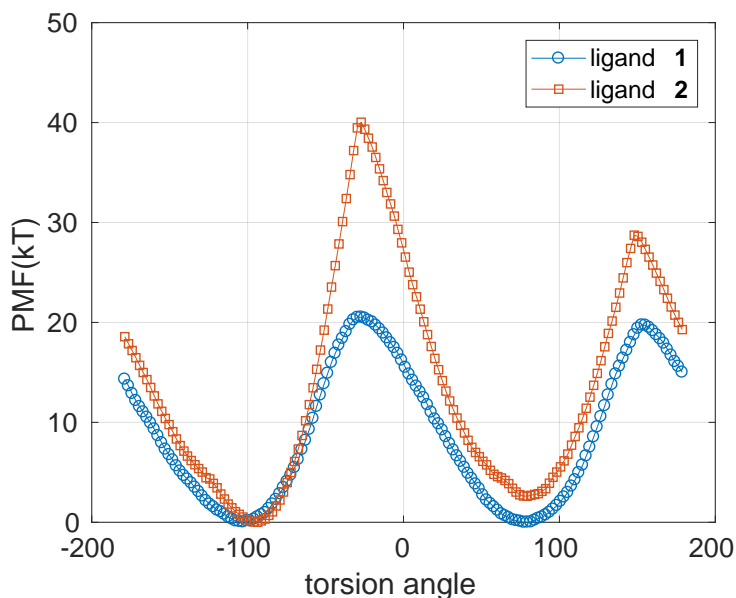


Figure S10. PMF as a function of the torsion angle of the rotatable bond present in ligands **1** and **2**, obtained using umbrella sampling simulations. Ligand **2** should ideally have a PMF similar to the ‘ideal’ one shown in Figure S8, since the two binding modes are equally populated. The protocol (optimized on ligand **1**) failed to reproduce the expected PMF for ligand **2**.

References

- (1) Gill, S. C.; Lim, N. M.; Grinaway, P. B.; Rustenburg, A. S.; Fass, J.; Ross, G. A.; Chodera, J. D.; Mobley, D. L. Binding Modes of Ligands Using Enhanced Sampling (BLUES): Rapid Decorrelation of Ligand Binding Modes via Nonequilibrium Candidate Monte Carlo. *J. Phys. Chem. B* **2018**, *122*, 5579–5598.
- (2) Kaus, J. W.; Harder, E.; Lin, T.; Abel, R.; McCammon, J. A.; Wang, L. How To Deal with Multiple Binding Poses in Alchemical Relative Protein–Ligand Binding Free Energy Calculations. *J. Chem. Theory Comput.* **2015**, *11*, 2670–2679.
- (3) van Zundert, G. C. P.; Hudson, B. M.; de Oliveira, S. H. P.; Keedy, D. A.; Fonseca, R.; Heliou, A.; Suresh, P.; Borrelli, K.; Day, T.; Fraser, J. S.; van den Bedem, H. qFit-ligand Reveals Widespread Conformational Heterogeneity of Drug-Like Molecules in X-Ray Electron Density Maps. *J. Med. Chem.* **2018**, *61*, 11183–11198.